Supporting Information

Highly active Fe sites in ultrathin pyrrhotite Fe_7S_8 nanosheets realizing efficient electrocatalytic oxygen evolution

Shichuan Chen[†], *Zhixiong Kang*[†], *Xiaodong Zhang*[*, †], *Junfeng Xie*[‡], *Hui Wang*[†], *Wei Shao*[†], *XuSheng Zheng*[§], *Wensheng Yan*[§], *Bicai Pan*[†] *and Yi Xie*[*, †]

[†]*Hefei National Laboratory for Physical Science at the Microscale, CAS Center for Excellence in Nanoscience, Collaborative Innovation Center of Chemistry for Energy Materials, University of Science and Technology of China, Hefei, 230026, P.R. China*

[‡]*College of Chemistry, Chemical Engineering and Materials Science, Shandong Normal University, Jinan, 250014, P. R. China*

[§]*National Synchrotron Radiation Laboratory, University of Science and Technology of China, Hefei, 230029, P.R. China*

*Corresponding Authors：zhxid@ustc.edu.cn; yxie@ustc.edu.cn

Experimental Section:

Synthesis of Fe_7S_8 bulk: Typically, 0.5 mmol $(NH_4)_3[Fe(C_2O_4)_3]\cdot 3H_2O$ and 1 mmol S were added into a mixed solution of 27 mL benzyl alcohol and 8 mL hydrazine hydrate (80%). After vigorous stirring for about 30 min, the mixture was then transferred into Teflon cup (50 mL) and heated in a sealed autoclave at 180 ^oC for 12 h. Upon cooling to room temperature, the precipitates were collected by centrifugation, washed with distilled water and absolute ethanol for several times and then dried under vacuum at 60 ^oC for 6 h.

Synthesis of Fe_7S_8-hexylamine intermediate: 0.5 mmol $(NH_4)_3[Fe(C_2O_4)_3]\cdot 3H_2O$ and 1 mmol S were added into a mixed solution of 27 mL benzyl alcohol and 8 mL hexylamine. After vigorous stirring for about 30 min, the mixture was then transferred into Teflon cup (50 mL) and heated in a sealed autoclave at 180 ^oC for 12 h. Upon cooling to room temperature, the precipitates were collected by centrifugation, washed with distilled water and absolute ethanol for several times and then dried under vacuum at 60 ^oC for 6 h.

Synthesis of Fe_7S_8 nanosheet: The Fe_7S_8 nanosheet was fabricated *via* a liquid exfoliation strategy. 50 mg Fe_7S_8-hexylamine intermediate was dispersed into N,N-Dimethylformamide (DMF) and then sonicated in ice water for 24 h. After sonicating treatment, the resultant dispersions were centrifuged at 2000 rpm for 10 min to remove the unexfoliated component. The target product was collected, then

thoroughly washed with deionized water and ethanol for at least five times, and then dried at 60 °C for 6 h under vacuum.

Synthesis of FeS nanosheet: 1 mmol $FeCl_2$ and 1 mmol Na_2S were added into a solution of 20 mL ethyl alcohol and 8 mL hexylamine. After vigorous stirring for about 30 min, the mixture was then transferred into Teflon cup (50 mL) and heated in a sealed autoclave at 160 ^oC for 12 h. Upon cooling to room temperature, the precipitates were collected by centrifugation, washed with distilled water and absolute ethanol for several times and then dried under vacuum at 60 ^oC for 6 h. Above precipitates were dispersed into DMF and then sonicated in ice water for 24 h. After sonicating treatment, the resultant dispersions were centrifuged at 2000 rpm for 10 min to remove the unexfoliated component. The target product was collected, then thoroughly washed with deionized water and ethanol for at least five times, and then dried at 60 °C for 6 h under vacuum.

Synthesis of FeOOH nanosheet: In a typical procedure,[1] 0.16 g $FeCl_3$, 0.08 g polyvinyl pyrrolidone (PVP: MWz 58 000) and 0.4 g NaOH were added into a solution of 20 mL water and 10 mL ethylene glycol solution. After vigorous stirring for about 30 min, the mixture was then transferred into Teflon cup (50 mL) and heated in a sealed autoclave at 120 ^oC for 12 h. Upon cooling to room temperature, the precipitates were collected by centrifugation, washed with distilled water and absolute ethanol for several times and then dried under vacuum at 60 ^oC for 6 h.

Material characterizations. The transmission electron microscopy (TEM) was observed with a JEOL JEM-ARM200F field emission electron microscope at an acceleration voltage of 200 kV. Atomic force microscopy (AFM) was measurement on the Veeco DI Nano-scope MultiMode V system. X-ray diffraction (XRD) spectra was recorded by Philips X'Pert Pro Super diffractometer with Cu-Kα radiation (λ=1.54178 Å). Raman spectra were acquired by a Renishaw RM3000 Micro Raman system. The Fourier transform infrared (FT-IR) spectra were detected on a MAGNA-IR 750 (Nicolet Instrument Co, U.S.). High-resolution transmission electron microscopy (HRTEM), the corresponding electron diffraction (ED) analyses, and HAADF-STEM images were carried out on a JEOL JEM-ARF200F. X-ray photoelectron spectra (XPS) were detected on the photoemission end-station at beamline BL10B in the National Synchrotron Radiation Laboratory (NSRL) in Hefei, China. The Fe L-edge synchrotron radiation-based X-ray absorption near edge structure (XANES) were measured at beamline BL12b of National Syncrotron Radiation Laboratory (NSRL, China) in the total electron yield (TEY) mode by collecting the sample drain current under a vacuum better than 5×10^{-8} Pa. The beam from the bending magnet was monochromatized utilizing a varied line-spacing plane grating and refocused by a toroidal mirror.

Electrochemical Measurements. All of the electrochemical measurements were performed in a three-electrode system on CHI770E electrochemical work station. In a typical procedure, 2 mg of electrocatalyst and 30 μL of 5 wt% Nafion solutions were dispersed in 1ml water/isopropanol solution (volume ratio = 3:1) by sonicating for at

least 40 min to form a homogeneous ink. Then, 5 μL of this solution was loaded onto a glassy carbon electrode (3 mm diameter) and dried naturally (loading 0.143 mg cm^{-2}). The electrochemical measurements of the samples at a scan rate of 5 mV/s were carried in 1 M KOH solution, using a Ag/AgCl electrode as the reference electrode and the platinum gauze as the counter electrode. All of the potentials were calibrated to an eversible hydrogen electrode (RHE) according to the Nernst equation: $E_{RHE} = E_{Ag/AgCl} + 0.059 \times pH + 0.1976$. The TOF is calculated from the equation: TOF = (J*A) / (4*F*m). Here, J (mA cm^{-2}) is the current density at a given overpotential. A is the surface area of the electrode, the number 4 means 4 electrons per mole of O_2. F is the Faraday constant (96485.3 C mol^{-1}), and m is the number of moles of metal on the electrode.[2, 3] Electrochemically active surface area (ECSA) was determined by Double-layer capacitance measurements. Cyclic voltammetry (CV) was investigated from 20 to 120 mV/s in 1.02~1.20 V vs. RHE. The double layer capacitance (C_d) was evaluated by plotting the Δj (j_a-j_c) at 1.15 V vs.RHE against the scan rates. The j_a and j_c are the anodic and cathodic current density, respectively. The slope is twice that of the double layer capacitance C_d. AC impedance measurements of the catalysts were measured with frequencies ranging from 100 kHz to 1 Hz, and the amplitude of the applied voltage was 5 mV.

Calculation method. The first-principles density functional theory (DFT) calculations were carried out with the projected augmented wave method with the Perdew-Burke-Ernzerhof (PBE) GGA functional encoded in the Vienna *ab initio* simulation package. The convergence on the choice of energy cut-off was tested to

300 eV, and the atomic positions were allowed to relax until the energy and force are less than 10^{-4} eV and -0.02 eV/Å, respectively. We optimized at the LSDA+U (U_{eff}=2 eV) for the correction of on-site Coulomb interaction, the lattice constant of the unit cell is in good agreement with experiment.[4-6]

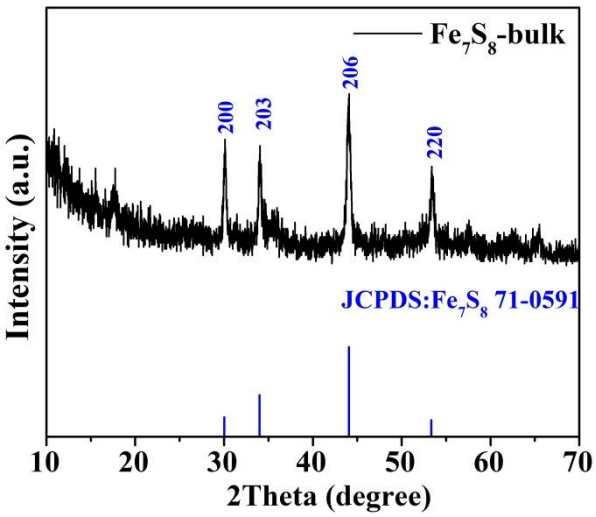

Figure S1. XRD pattern of Fe_7S_8-bulk.

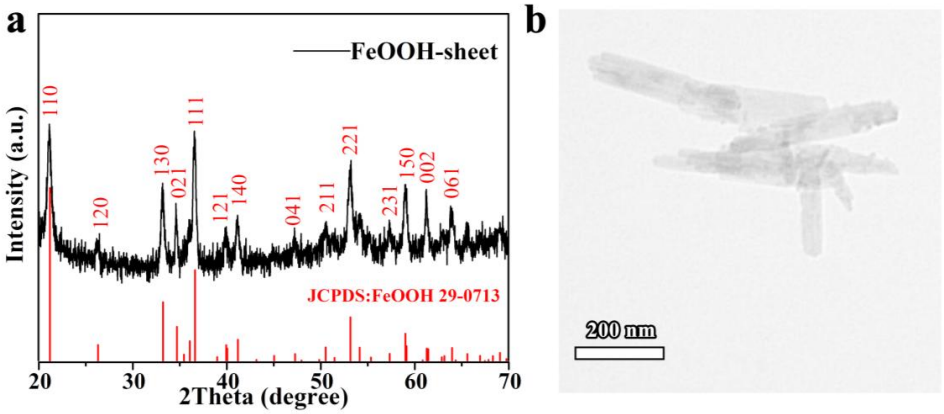

Figure S2. (a) XRD pattern of FeOOH-sheet. (b) TEM image of FeOOH-sheet.

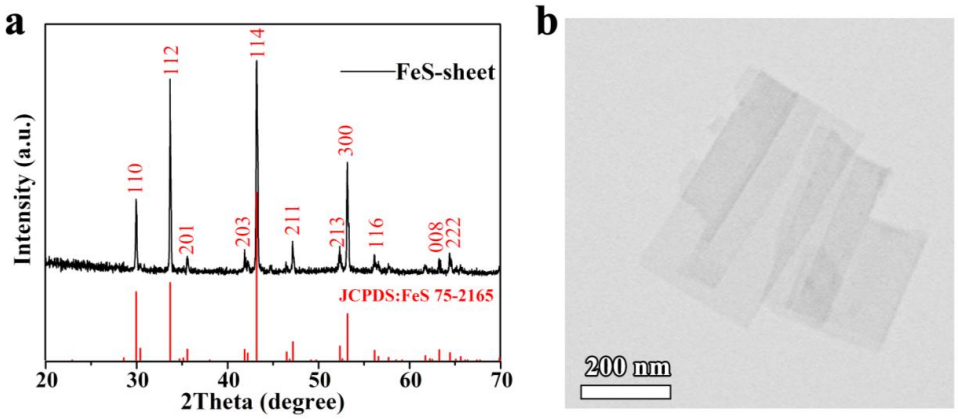

Figure S3. (a) XRD pattern of FeS-sheet. (b) TEM image of FeS-sheet

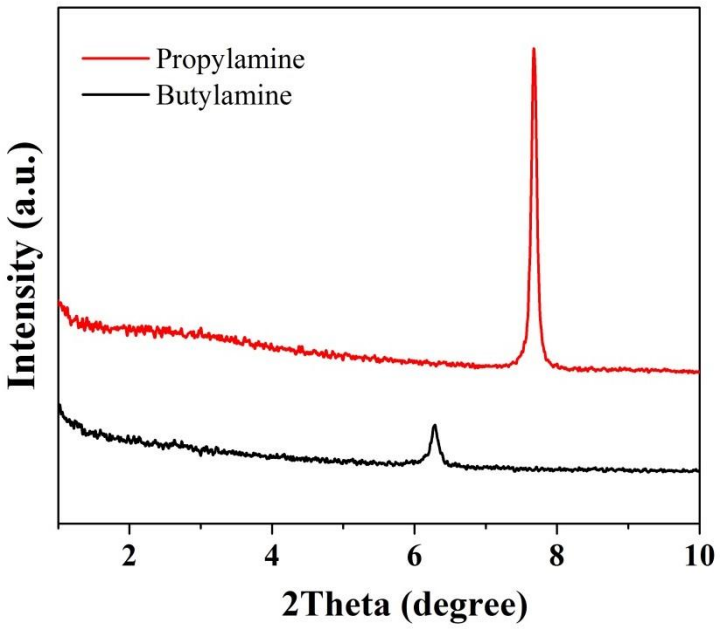

Figure S4. Small-angel XRD patterns of Fe_7S_8-amine intermediate with different chain lengths.

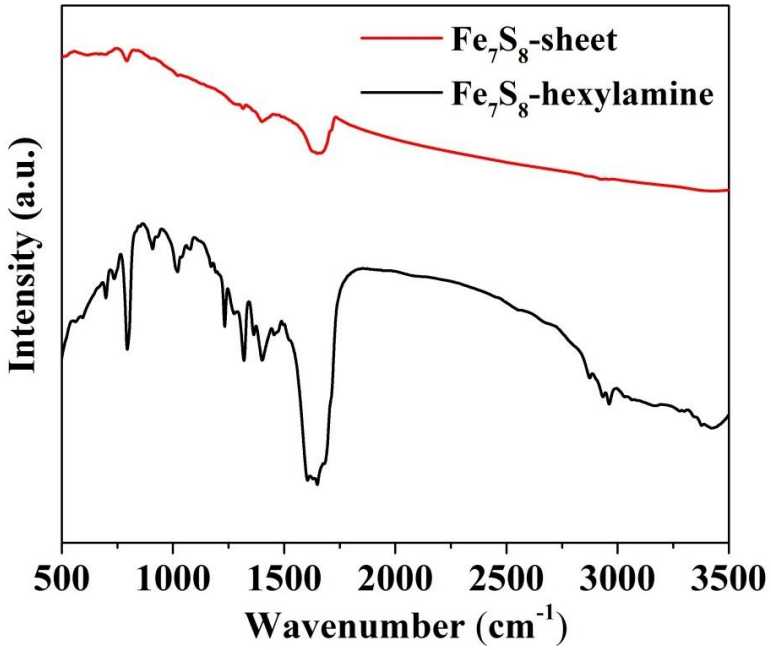

Figure S5. IR spectra of Fe_7S_8 nanosheet and Fe_7S_8-hxylamine. The vibration bands suggest the existence of amine in Fe_7S_8-hexylamine intermediate. After exfoliation, the vibration bands of amine are absent, indicating the clean surface of the Fe_7S_8 nanosheet.

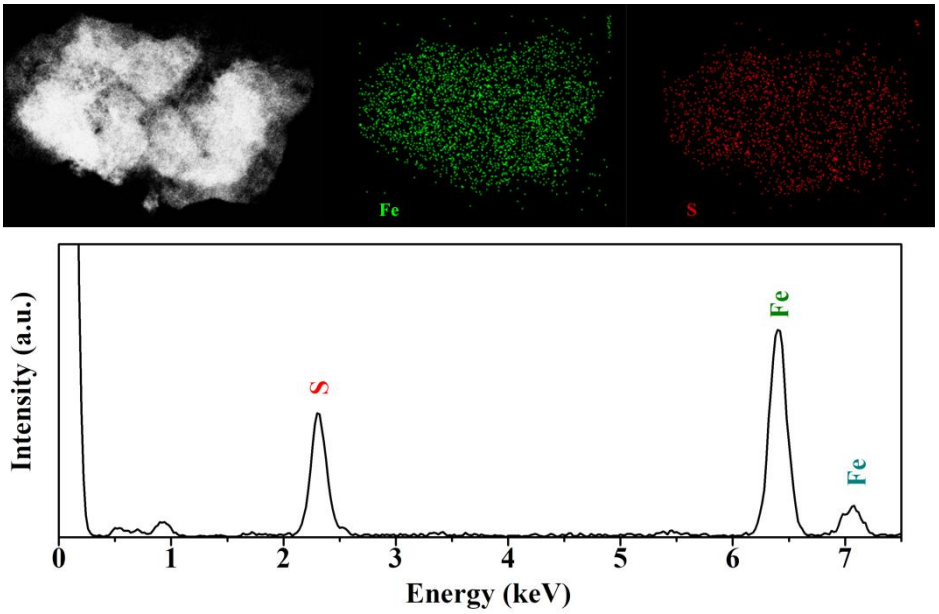

Figure S6. EDX mapping analyses of Fe_7S_8-nanosheet, which indicates the homogeneously distributed Fe and S in the Fe_7S_8-nanosheet.

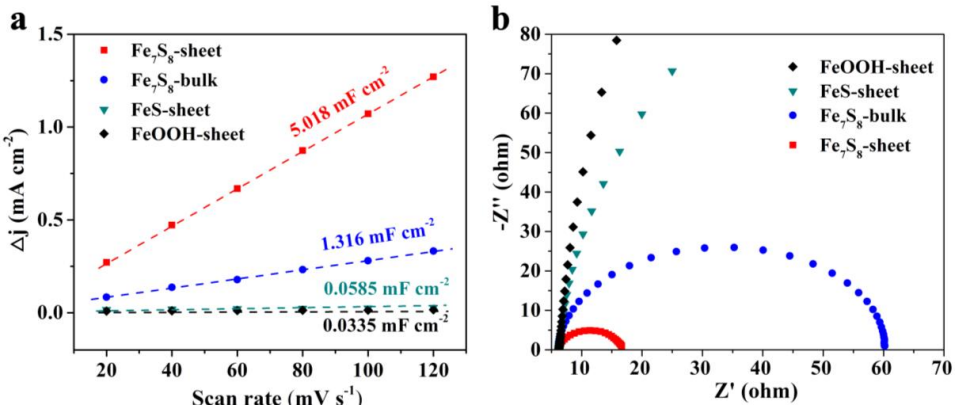

Figure S7. (a) The difference in current density variation plotted against scan rate fitted to a linear regression enables the estimation of C_{dl}; (b) Nyquist plots of samples.

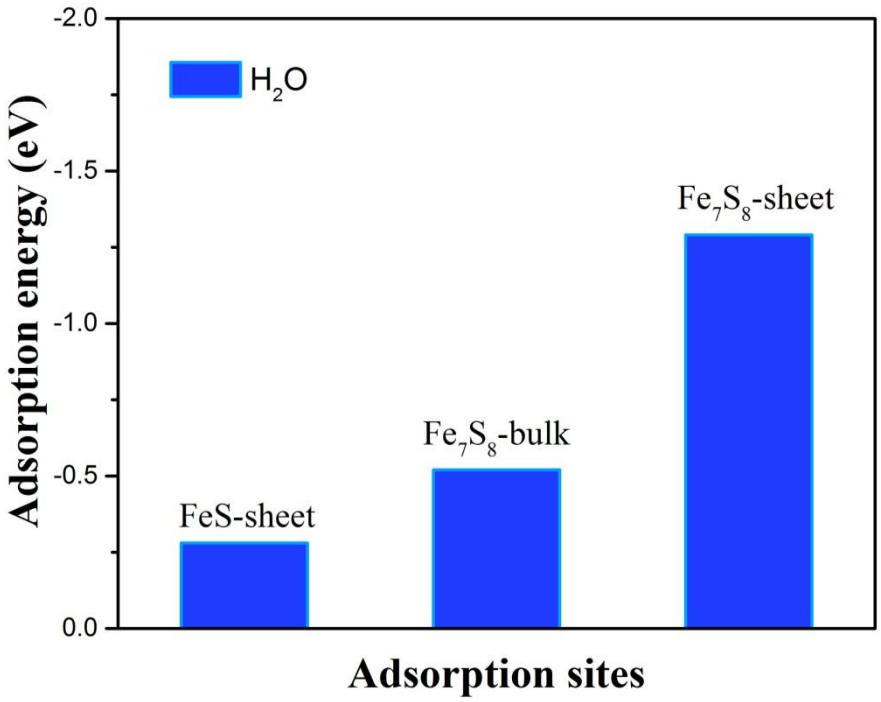

Figure S8. Calculated adsorption energy for FeS-bulk, Fe_7S_8-bulk and Fe_7S_8-nanosheet.

Table S1. Summary of the electrochemical properties of electrocatalysts

Catalyst	overpotential (η) (at 10 mA cm^{-2})	j,η=0.50 V/mA cm^{-2}
Fe_7S_8 nanosheets	0.27	300.0
Fe_7S_8 bulk	0.38	56.1
FeS –sheet	0.55	2.74
FeOOH	0.56	1.54
RuO_2	0.25	185.2

Table S2. Comparison of electrocatalytic activity of Fe-based OER catalysts.

Catalyst	overpotential (η) (at 10 mA cm^{-2})	j,η=0.35 V/mA cm^{-2}	Ref
Fe_7S_8 nanosheets	0.27	58.5	This work
Fe_7S_8 bulk	0.38	6.6	This work
FeOOH	0.50	0.1	(7)
FeO_x	0.41	0.2	(8)
NiFe LDH	0.32	5.5	(9)
$NiFeO_x$	0.35	15	(10)
$Fe_{0.5}V_{0.5}$ hydroxide	0.29	7.5	(11)

References:

(1) Zhai, Y.; Ma, X.; Mao, H.; Shao, W.; Xu, L.; He, Y.; Qian, Y. Mn-Doped α-FeOOH Nanorods and α-Fe_2O_3 Mesoporous Nanorods: Facile Synthesis and Applications as High Performance Anodes for LIBs. *Adv. Electron. Mater.* **2015,** *1*, 1400057.

(2) Liu, Y.; Xiao, C.; Lyu, M.; Lin, Y.; Cai, W.; Huang, P.; Tong, W.; Zou, Y.; Xie, Y. Ultrathin Co_3S_4 nanosheets that synergistically engineer spin states and exposed polyhedra that promote water oxidation under neutral conditions. *Angew. Chem. Int. Ed.* **2015,** 54, 11231-11235.

(3) Huang, J.; Chen, J.; Yao, T.; He, J.; Jiang, S.; Sun, Z.; Liu, Q.; Cheng, W.; Hu, F.; Jiang, Y.et al. CoOOH Nanosheets with High Mass Activity for Water Oxidation. *Angew. Chem. Int. Ed.* **2015,** 54, 8722-8727.

(4) Kresse, G.; Joubert, D. From ultrasoft pseudopotentials to the projector augmented-wave method. *Phys. Rev. B.* **1999,** *59*, 1758-1775.

(5) Perdew, J. P.; Burke, K.; Ernzerhof, M. Generalized gradient approximation made simple. *Phys. Rev. Lett.* **1996,** *77*, 3865-3868.

(6) Bao, J.; Zhang, X.; Fan, B.; Zhang, J.; Zhou, M.; Yang, W.; Hu, X.; Wang, H.; Pan, B.; Xie, Y. Ultrathin Spinel-Structured Nanosheets Rich in Oxygen Deficiencies for Enhanced Electrocatalytic Water Oxidation. *Angew. Chem. Int. Ed.* **2015,** *54*, 7399-7404.

(7) Lyons, M. E.; Brandon, M. P. Redox switching and oxygen evolution electrocatalysis in polymeric iron oxyhydroxide films. *Phys. Chem. Chem. Phys.* **2009,** *11*, 2203-2217.

(8) Trotochaud, L.; Ranney, J. K.; Williams, K. N.; Boettcher, S. W. Solution-cast metal oxide thin film electrocatalysts for oxygen evolution. *J. Am. Chem. Soc.* **2012,** *134*, 17253-17261.

(9) Gong, M.; Li, Y. G.; Wang, H. L.; Liang, Y. Y.; Wu, J. Z.; Zhou, J. G.; Wang, J.; Regier, T.; Wei, F.; Dai, H. J. An Advanced Ni-Fe Layered Double Hydroxide Electrocatalyst for Water Oxidation. *J. Am. Chem. Soc.* **2013,** *135*, 8452-8455.

(10) McCrory, C. C.; Jung, S.; Peters, J. C.; Jaramillo, T. F. Benchmarking heterogeneous electrocatalysts for the oxygen evolution reaction. *J. Am. Chem. Soc.* **2013,** ***135,*** 16977-16987.

(11) Fan, K.; Ji, Y.; Zou, H.; Zhang, J.; Zhu, B.; Chen, H.; Daniel, Q.; Luo, Y.; Yu, J.; Sun, L. Hollow Iron-Vanadium Composite Spheres: A Highly Efficient Iron-Based Water Oxidation Electrocatalyst without the Need for Nickel or Cobalt. *Angew. Chem. Int. Ed.* **2017,** *56*, 3289-3293.